CGMS IPWG

International Precipitation Working Group

Proceedings

1st Workshop

Madrid, Spain

23-27 September 2002

NOAA INM EUMETSAT

IMPACTS OF IMPROVED ERROR ANALYSIS ON THE ASSIMILATION OF POLAR SATELLITE PASSIVE MICROWAVE PRECIPITATION ESTIMATES INTO THE NCEP GLOBAL DATA ASSIMILATION SYSTEM

Robert J. Kuligowski[1], Russ Treadon[2], and W. Chen[3]

Abstract

Numerous authors have demonstrated that assimilating precipitation observations into a numerical weather prediction (NWP) model positively impacts model forecasts via improving the specification of water content and latent heat release, particularly over oceanic regions where data from other sources are scarce. However, the initial impacts of assimilating rain rate estimates from the Special Sensor Microwave/Imager (SSM/I) and the Tropical Rainfall Measuring Mission (TRMM) Microwave Imager (TMI) into the Global Data Assimilation System (GDAS) was minimal, especially in comparison to the impact of changes to the model physics around the same time. In this work, the assimilation of SSM/I rain rates into the GDAS is modified using a more rigorous error analysis, and the preliminary impacts are discussed.

1. Background

Precipitation is highly important in numerical weather prediction (NWP), not only as a predicted variable, but also because precipitation-related processes feed back into other atmospheric fields via evaporation, latent heat release, and other means. However, numerical model predictions of precipitation have been quite poor, in part because of deficiencies in the model representation of the appropriate processes, but also because of the difficulty in obtaining atmospheric moisture information on the fine temporal and spatial scales that are needed.

The objective of precipitation assimilation is to improve NWP model performance by minimizing the differences between simulated and observed precipitation during model initialization. One approach to doing so is to invert the model convective parameterization and nudge the inputs (e.g. vertical profiles of temperature and water vapor content) in order to get the resulting rain rates to match the target values (e.g. Mathur et al., 1992). This approach has proven to be quite useful in tropical regions where the majority of precipitation is convective in nature.

Another approach is to use variational techniques (e.g. Lorenc, 1986; Parrish and Derber, 1992). In this type of approach, the error-weighted difference between simulated and observed precipitation is expressed as a cost function that must be minimized. This function is minimized in a stepwise fashion whereby its local gradient is determined, the model variables are then modified

[1] Center for Satellite Applications and Research, NOAA/NESDIS, E/RA2, RM 601 WWB, 5200 Auth Rd., Camp Springs, MD 20746-4308, USA
[2] Environmental Modeling Center, NOAA/NWS/NCEP, W/NP2 RM 207 WWB, 5200 Auth Rd., Camp Springs, MD 20746-4308, USA
[3] Caelum Research Corporation, 1700 Research Boulevard, Suite 100, Rockville, MD 20850, USA

in the direction of the downward local gradient, and a new local gradient is determined until the minimum value is reached. To approximate this gradient in a local sense, the model precipitation physics are expressed as an operator that maps the analysis variables to the location, time, and type of observation, and the adjoint of this operator provides the required gradient information.

The Environmental Modeling Center (EMC) of the National Centers for Environmental Prediction (NCEP) currently assimilate rain rate estimates from two polar-orbiting satellite instruments into Global Data Assimilation System (GDAS) via variational techniques. Estimates from the Special Sensor Microwave/Imager (SSM/I) based on the algorithms of Ferraro (1997) have been assimilated since February 2001, while estimates from the Tropical Rainfall Measuring Mission (TRMM) Microwave Imager (TMI) from the Kummerow et al. (2001) algorithm have been assimilated since October 2001.

Around the same time, a new physics package was introduced into the NCEP Global Forecast System (GFS), based on the scheme developed by Zhao and Carr (1997). This scheme includes explicit prognostic cloud water and ice and its effects on its surroundings (e.g. radiation, detrainment outside the cloud).

A comparison of the impact of the microwave-based rain rate assimilation to the impact of the new physics package was conducted using data from August 1999. The control model using the old physics and no microwave-based rain rate assimilation (“Control-00”) was compared to both the GFS with the 2001 physics and no microwave-based rain rate assimilation (“Control-01”) and the GFS with microwave-based rain rate assimilation (and the previous physics package). Furthermore, two variations of the latter were performed: one where the rain rates were used to adjust the coldest cold in the ensemble (“Single-cloud”), and one where a randomly selected cloud in the ensemble was selected (“Multi-cloud”).

The results showed that the assimilation of microwave-based rain rates had little impact on both the assimilation fields (Fig. 1) and on the forecast fields (Fig. 2) compared to the impact of the change in physics. The new physics package led to significant improvements in the representation of water vapor (q) and in rainfall rates compared to the SSM/I and TRMM-based estimates in the initialization, while the data assimilation generally produced neutral to slightly negative impacts. The northern hemisphere height fields also exhibited significant improvement with the new physics package, especially in the medium range, while the impact of the rain rate assimilation was again neutral to slightly negative.

The most likely reasons for limited impact are twofold. The first is the difficulty in using a linear adjoint as an approximation to the local slope of a highly nonlinear cost function such as that associated with the GFS precipitation physics. The second reason is that a detailed error analysis of the SSM/I and TRMM rain rates was not available when assimilation of these fields began. Uncertainty in the error characteristics of any input data set leads to an excessively low weighting of that observation within the analysis system in order to prevent detrimental impacts from errors in that data set.

2. Error analysis

This work deals with the first problem—that of inadequate weighting of the microwave rain rate estimates in the assimilation due to a lack of error information. The error analysis was performed for the period April-October 2001, by comparing SSM/I rain rate estimates to Stage III radar/raingauge fields (Fulton et al., 1998) over the continental United States, with the latter serving as “ground truth” for this particular study. Though the Stage III estimates are considered to be less accurate than raingauge data because of radar-related errors (e.g. Young et al., 1999), their continuous spatial coverage made them highly desirable for this particular application. The direct comparison of instantaneous rain rate estimates from the SSM/I to hourly amounts from Stage III was another problem; but again, it was disregarded since the Stage III data offered by far the largest quality dataset of its kind for comparison to the SSM/I data. To avoid the significant problems associated with Stage III estimates in areas of high-relief terrain (e.g. Westrick et al., 1999, Young et al., 2000), the error analysis was performed only for regions east of longitude 105 W. In order to produce comparisons that were appropriate for use in the GDAS, both the SSM/I rain rates and the Stage III radar/raingauge fields were aggregated onto the GFS Gaussian grid (triangular truncation at total wave number 126, which is equivalent to approximately 100-km resolution at the equator).

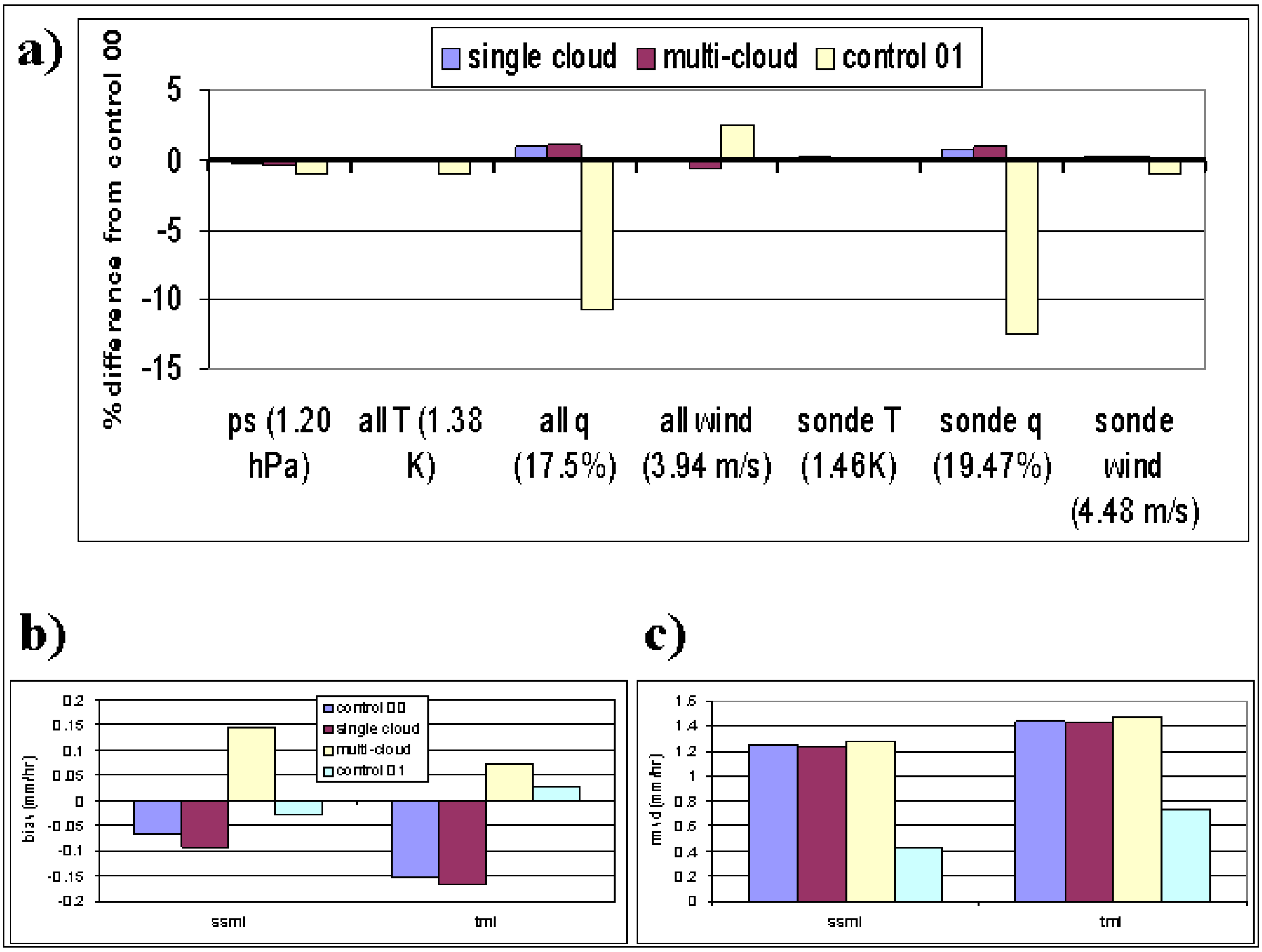

Figure 1. *Impact of microwave rain rate assimilation on the GFS initialization during 15-18 August 1999. The percent change of several variables from the control run value (in parentheses below the variable name) is shown in (a); (b) shows the bias of the four runs compared to both SSM/I and TRMM data as "ground truth"; and (c) shows the root-mean-squared difference (RMSD) from the same two data sets. The names of the model runs are explained in Section1 of the text.*

The objective of the analysis was to obtain expressions of both the error and the error uncertainty as a function of SSM/I rain rate, with error in this case referring to the ratio of estimated to observed amount. However, since the precipitation distribution is highly skewed, the analysis was performed on a ln(n+1) scale to obtain a more Gaussian distribution (the addition of 1 was required to avoid errors associated with zero rainfall). Separate analyses were performed for each algorithm type (scattering over land, emission over ocean, etc.) in order to produce the most robust error analysis possible.

Since both estimates of error and of error uncertainty were required, the data were sorted in order of ascending SSM/I rain rate and then binned into groups of 50. Computing the ratio mean and standard deviation for each of these bins resulted in compatible estimates of both error and error uncertainty. The resulting analyses are illustrated by the scatterplots in Fig. 2, where the values (and best-fit line) are indicated by gray dots, the bin means (and best-fit line) are in blue, and the bin standard deviations (and best-fit line) are in red. Note that in all cases, the SSM/I estimates exhibit a dry bias for very low rates (ln<0, so bias<1), but a wet bias that increases with SSM/I rain rate. Both the error and the uncertainty are approximated quite well using linear functions.

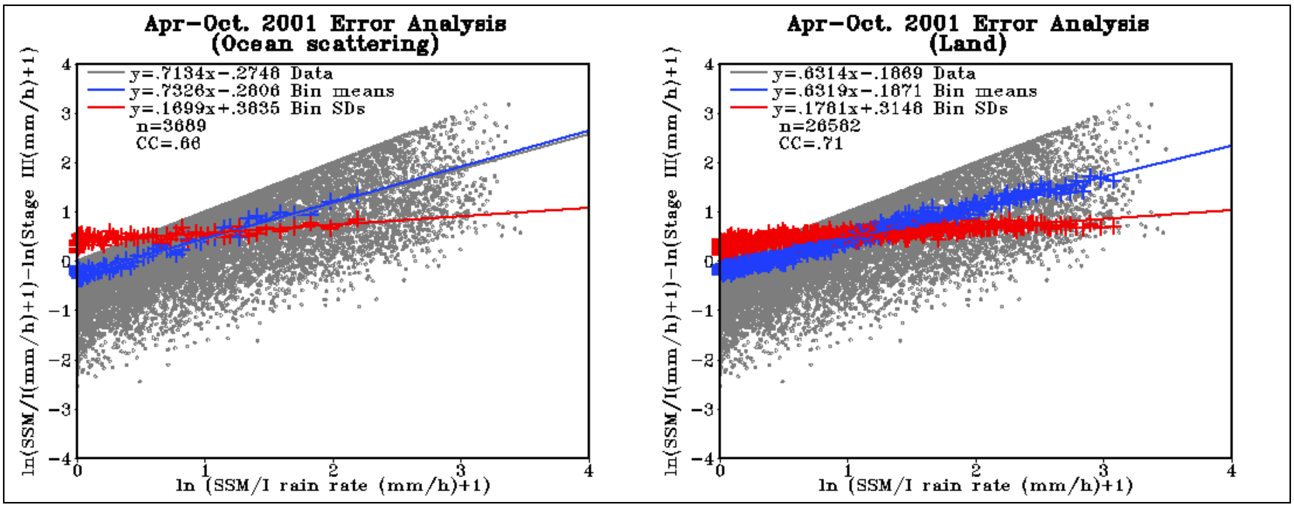

Figure 2. *Error analysis of rain rates from the SSM/I for the ocean scattering (left) and land (right) algorithms. The grey points represent values (on a log(n+1) scale; the mean values for the 50-point bins (see text) are blue crosses (with a blue best-fit line), while the bin standard deviations and best-fit line are in red. The value of n indicates the number of data points used in the analysis, while the value of CC is the linear correlation coefficient between the SSM/I and Stage III data.*

3. Assimilation scheme

The GDAS uses an intermittent assimilation system with a 6-hourly ingest cycle (0000, 0600, 1200, and 1800 UTC); estimates within ±3 hours of the analysis time are used in the assimilation. The SSM/I rain rates are converted to "superobs" (a non-weighted average onto a 1-degree lat/lon grid) for assimilation, and approximately 7,600 such superob rain rates from the 60°S-60°N latitude band are used in each analysis cycle.

The cost function used in this 3-D variational technique is expressed as follows:

$$2\,J(x_a) = (x_b-x_a)^T\,\mathbf{B}^{-1}\,(x_b-x_a) + (y_{obs} - R(x_a))^T\,\mathbf{O}^{-1}\,(y_{obs} - R(x_a)) + (J_{div} + J_q) \qquad (1)$$

where x_a represents the analysis variables, x_b is the best estimate of the current state of the atmosphere, and y_{obs} represents the assimilated observations. For precipitation, $R(x_a)$ is the operator which transforms the analysis state to the observation according to type, location, and time. The adjoint of this operator provides gradient information used by the minimization algorithm. **B** is the error covariance matrix from the background state (computed by comparing corresponding 24-h and 48-h forecasts); the lower the value of **B**, the less that the data will be allowed to change the background during initialization. **O** is the error covariance matrix for the observation and the forward model (computed using the error uncertainty analysis from the previous section). J_{div} and J_q are additional constraints placed on the analysis state.

The observation error O for rain rates is expressed as:

$O = O_{rep} + \max [O_{ssmi}, \alpha O_{ssmi} + (1-\alpha) O_{mod}]$

where O_{rep} is the representativeness error (the error from inconsistencies in time and space scales between the observations and the output of the forward model—arbitrarily set to 0.1), O_{ssmi} is the error uncertainty (i.e. the equation of red line from Fig. 2 after conversion back into linear space), and O_{mod} is the forward model error, which is estimated by comparing the model rain rates computed from the background (analysis) field at the location of the SSM/I observations. The value of α is set at a constant value of 0.5.

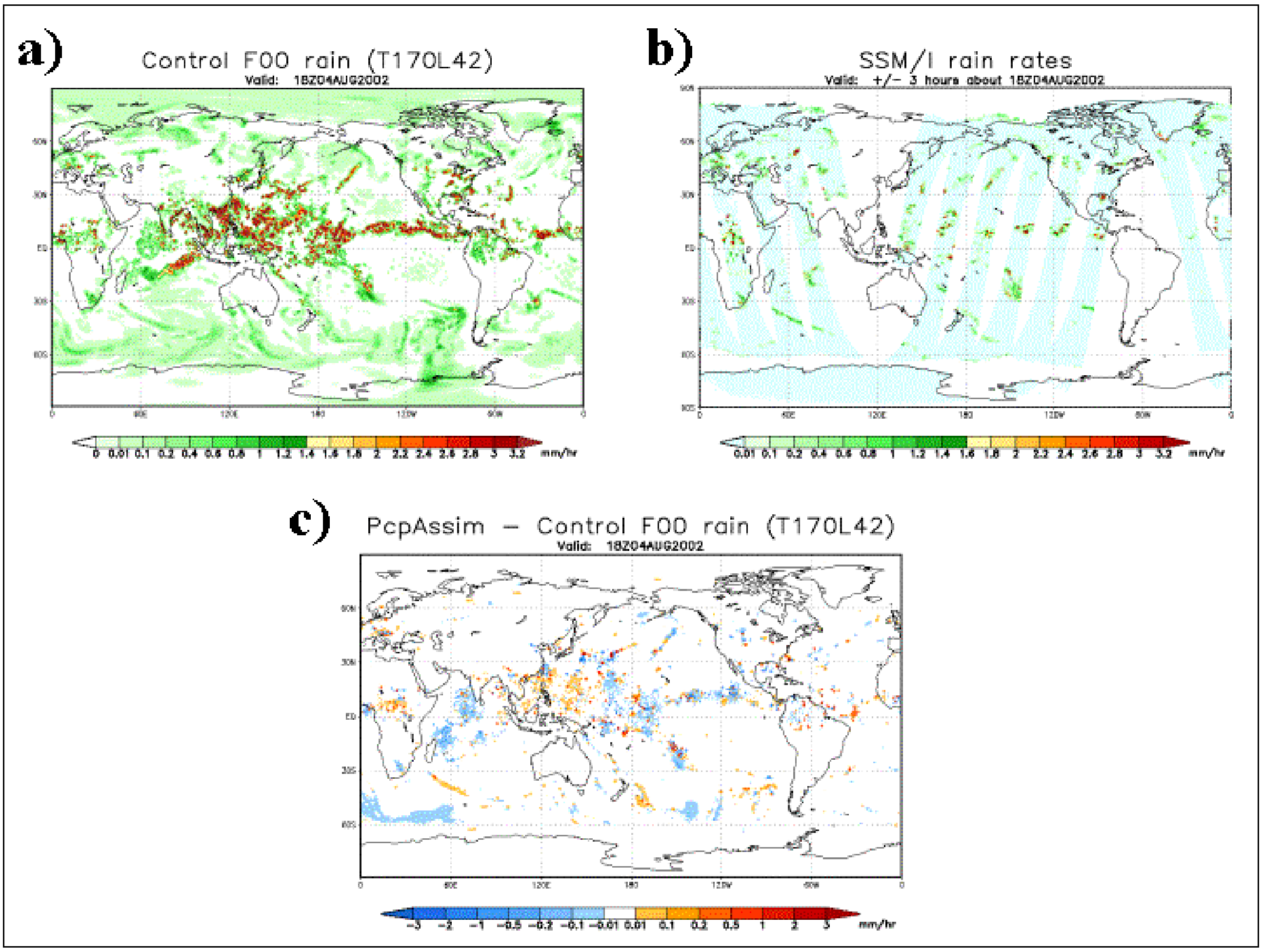

Figure3. *Comparison of the control GFS initial rain rate field valid 1800 UTC 4 August 2002 (a) with the corresponding SSM/I rain rate field (b). The difference between the initial rain rate field for the GFS with and without (control) SSM/I rain rate assimilation is shown in (c).*

4. Preliminary results

As shown in Fig. 3(a-c), the impact on the analysis is rather small, though excessive precipitation is reduced in portions of both the tropics and extratropics. The aforementioned difficulties arising from using linear adjoints to approximate the extremely nonlinear error functions related to the the GFS model physics makes enhancements of light rainfall rates more difficult to achieve than reduction of excessive rainfall rates. Figure 4 illustrates that the impact tends to be restricted to the total precipitable water (TPW) and water vapor (q) fields for the test period of 27 July to 5 August 2002. A slight positive impact in the forecasts was seen during this period for the northern (summer) hemisphere, while the impact in the Southern (winter) Hemisphere was neutral. However, all of these results are preliminary, as only global measures have been examined thus far where regional positive and negative impacts tend to cancel each other out. It is possible that as closer examination is performed, patterns of more significant impact may be observed.

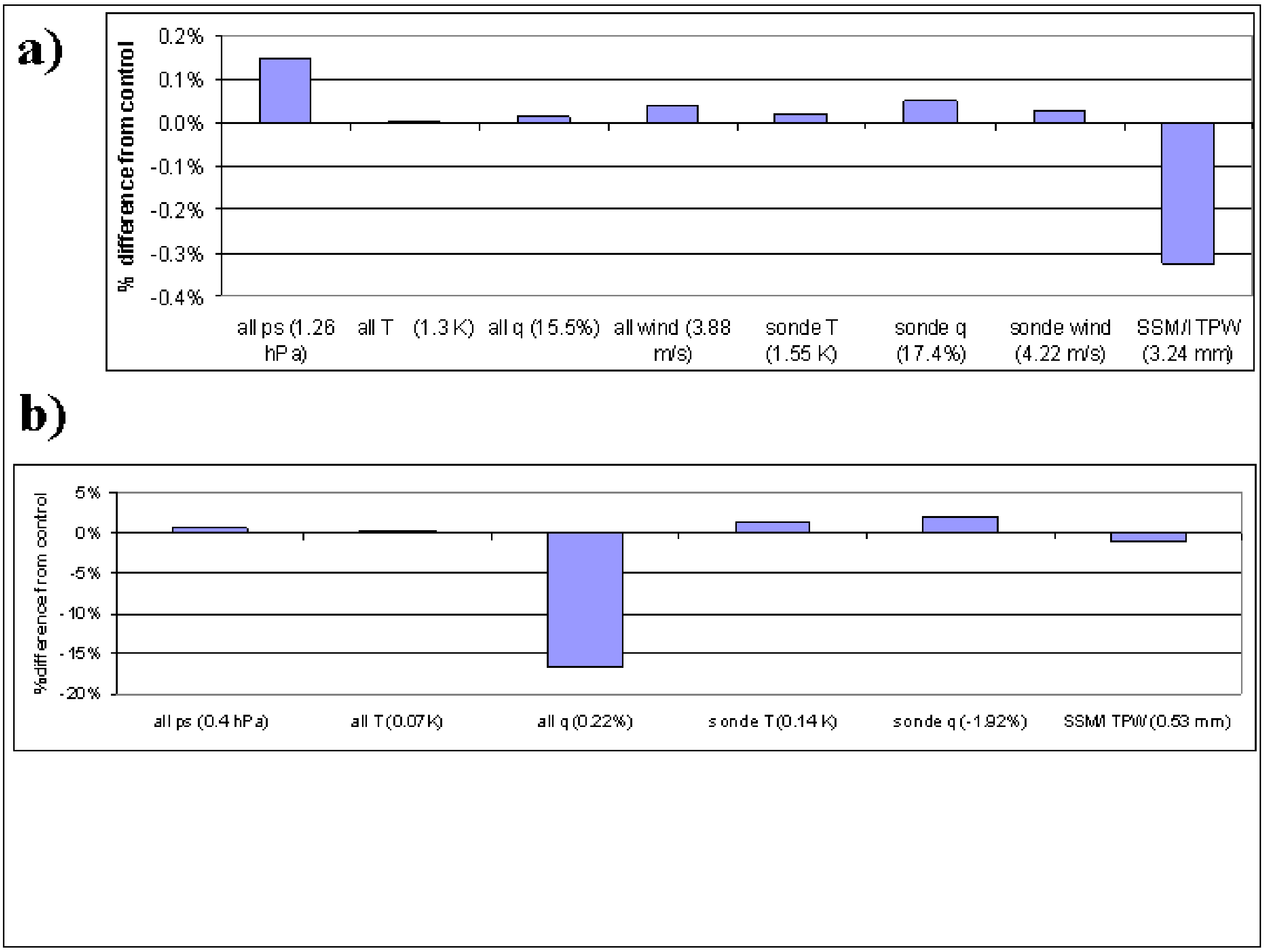

Figure4. *Impact of the new microwave rain rate assimilation on the GFS initialization during 27 July-5 August 2002. The bars in (a) show the percent change of root mean squared difference (RMSD) from the control run (in parentheses below the variable name) to the assimilation run; (b) is for bias instead of RMSD.*

5. Future work

A corresponding error analysis of rain rates from the Advanced Microwave Sounding Unit (Ferraro et al., 2000) has been performed (Fig. 5) in preparation for assimilation experiments for that instrument. However, evidence of larger differences between the SSM/I and AMSU rain rates over the tropics will have to be investigated before proceeding.

Additional avenues for future work include modifying the forward model and exploring alternatives to the current moisture analysis variable. Simplifying the physics of the forward model (while maintaining the essential features) would result in a less non-linear error function and thus reduce the errors associated with applying linear adjoints in the error minimization scheme. Regarding the moisture analysis variable, its large dynamic range (several orders of magnitude from the surface to the top of the atmosphere) and phase changes compromise its suitability as an analysis variable. Furthermore, a multivariate expression of atmospheric moisture, if possible, would permit a greater degree of constraint in the error minimization process.

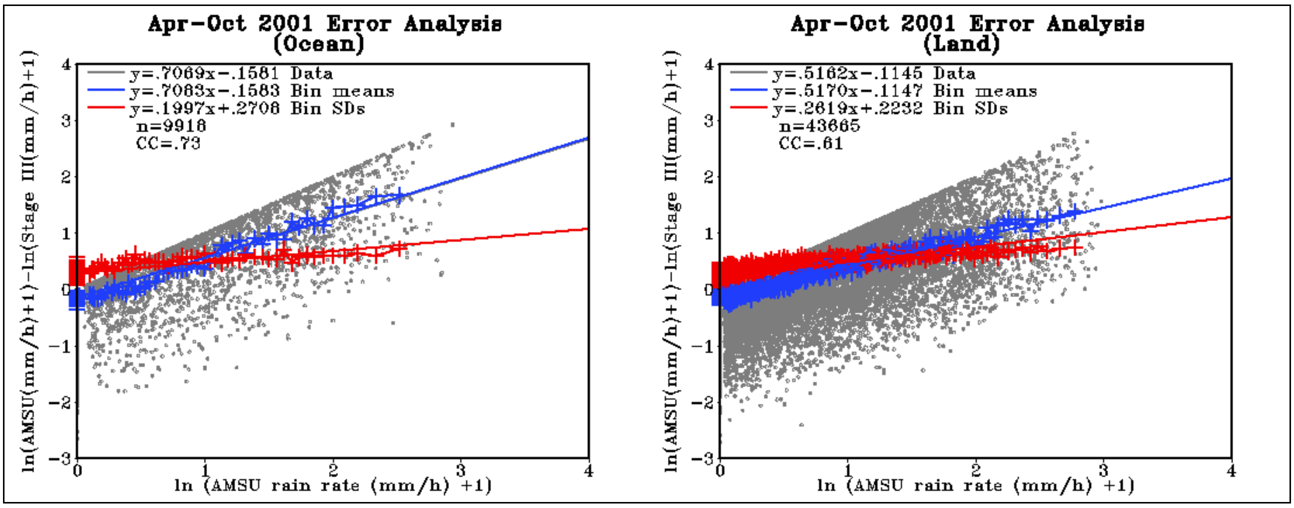

Figure5. *Same as in Figure 2, but for the AMSU.*

6. References

Ferraro, R. R., 1997: Special Sensor Microwave Imager derived global rainfall estimates for climatological applications. *J. Geophys. Res.*, **102**, 16715-16736.

Fulton, R. A., J. P. Breidenbach, D. J. Seo, and D. A. Miller, 1998: The WSR-88D rainfall algorithm. *Wea. Forecasting*, **13**, 377-395.

Kummerow, C. Y. Hong, W. S. Olson, S. Yang, R. F. Adler, J. McCollum, R. Ferraro, G. Petty, D. B. Shin, and T. T. Wilheit, 2001: The evolution of the Goddard Profiling Algorithm (GPROF) for rainfall estimation from passive microwave sensors. *J. Appl. Meteor.*, **40**, 1801-1820.

Lorenc, A. C., 1986: Analysis methods for numerical weather prediction. *Q. J. R. Meteor. Soc.*, **112**, 1177-1194.

Mathur, M. B., H. S. Bedi, T. N. Krishnamurti, M. Kanamitsu, and J. S. Woollen, 1992: Use of satellite-derived rainfall for improving tropical forecasts. *Mon. Wea. Rev.*, **120**, 2540-2560.

Parrish, D. F., and J. C. Derber, 1992: The National Meteorological Center's Spectral Statistical-Interpolation Analysis System. *Mon. Wea. Rev.*, **120**, 1747-1763.

Westrick, K. J., C. F. Mass, and B. A. Colle, 1999: The limitations of the WSR-88D radar network for quantitative precipitation measurement over the coastal western United States. *Bull. Amer. Meteor. Soc.*, **80**, 2289-2298.

Young, C. B., A. A. Bradley, W. F. Krajewski, A. Kruger, and M. L. Morrissey, 2000 Evaluating NEXRAD multisensor precipitation estimates for operational hydrologic forecasting. *J. Hydrometeorology*, **1**, 241-254.

——————, B. R. Nelson, A. A. Bradley, J. A. Smith, C. D. Peters-Lidard, A. Kruger, and M. L. Baeck, 1999: An evaluation of NEXRAD precipitation estimates in complex terrain. *J. Geophys. Res.*, **104 (D16)**, 19691-19703.

Zhao, Q., and F. H. Carr, 1997: A prognostic cloud scheme for operational NWP models. *Mon. Wea. Rev.*, **125**, 1931-1953.